Dalton Transactions

PAPER

View Article Online
View Journal

Cite this: DOI: 10.1039/c5dt02685g

Biomimetic ferrichrome: structural motifs for switching between narrow- and broad-spectrum activities in *P. putida* and *E. coli*†

Evgenia Olshvang,‡[a] Agnieszka Szebesczyk,‡[b] Henryk Kozłowski,[b] Yitzhak Hadar,[c] Elzbieta Gumienna-Kontecka*[b] and Abraham Shanzer*[a]

Received 15th July 2015,
Accepted 3rd September 2015

DOI: 10.1039/c5dt02685g

www.rsc.org/dalton

A series of novel ferrichrome (FC) analogs was designed based on the X-ray structure of FC in the FhuA transporter of *Escherichia coli*. Two strategies were employed: the first strategy optimized the overall size and relative orientation of H-bonding interactions. The second strategy increased H-bonding interactions by introducing external H-donors onto analogs' backbone. Tris-amino templates were coupled to succinic or aspartic acid, and the second carboxyl was used for hydroxamate construction. Succinic acid provided analogs without substituents, whereas aspartic acid generated analogs with external amines (*i.e.* H-donors). All analogs had similar physicochemical properties, yet the biological activity in *Pseudomonas putida* and *E. coli* showed great variation. While some analogs targeted specifically *P. putida*, others were active in both strains thus exhibiting broad-spectrum activity (as in native FC). Narrow-spectrum or species-specificity might find application in microbial diagnostic kits, while broad-spectrum recognition may have advantages in therapeutics as siderophore–drug conjugates. The differences in the structure and range of microbial recognition helped us in formulating guidelines for minimal essential parameters required for inducing broad-spectrum activity.

Introduction

Iron is an essential trace metal for virtually all life forms,[1–3] and crucial for a wide variety of cell functions, ranging from oxygen metabolism and electron transfer processes to DNA and RNA synthesis. However, under the oxidizing earth atmosphere iron forms insoluble hydroxyl polymers inaccessible to microorganisms.

To obtain iron, microorganisms have developed a unique iron acquisition system that strictly controls iron uptake.[4–6] It consists of (i) bio-synthesis and secretion of iron chelators, called siderophores,[7] capable of solubilizing and sequestering iron from ferric hydroxyl polymers, and (ii) a specific transport system that recognizes the siderophore-iron complex and transports it into the cytoplasm.[8–13]

Ferrichrome[14–16] (FC; Chart 1a) is a prototype of the natural hydroxamate siderophores. It is composed of a chiral hexapeptide ring template, non-symmetrically extended by three identical arms that are terminated by hydroxamate moieties. FC, similarly to most siderophores, is not species-specific; it exhibits broad-spectrum activity and thus can be recognized by various types of microorganisms.[17,18] Among the various proteins that control FC transport inside the cell, the outer membrane transporter is responsible for the selective recognition of FC.[19,20] Ferric hydroxamate uptake protein component A (FhuA) is a FC transporter from the outer membrane of *Escherichia coli* and is among the few membrane transporters with a resolved crystal structure.[21,22] The crystallographic data indicate the presence of two sets of H-bonding networks that dominate the recognition process. The first H-bonding network links between the oxygen of the hydroxamate groups and proton-donors within the transporter, and the second network connects the amide-carbonyls in the FC peptidic skeleton with the transporter.

Biomimetic chemistry is a discipline that aims to mimic or reproduce biological activity, rather than reproduce the detailed structure of a substrate.[23–26] Extensive studies on biomimetic tris-hydroxamate siderophores[27–30] established that: (i) the cyclic hexapeptide ring of FC can be replaced by a C3 symmetric template;[31–33] and (ii) the presence of the hydrox-

[a]Department of Organic Chemistry, The Weizmann Institute of Science, Rehovot 76100, Israel. E-mail: abraham.shanzer@weizmann.ac.il
[b]Faculty of Chemistry, University of Wrocław, F. Joliot-Curie 14, 50-383 Wrocław, Poland. E-mail: elzbieta.gumienna-kontecka@chem.uni.wroc.pl
[c]Department of Plant Pathology and Microbiology, The R.H. Smith Faculty of Agriculture Food and Environment, The Hebrew University of Jerusalem, Rehovot 76100, Israel

†Electronic supplementary information (ESI) available. See DOI: 10.1039/c5dt02685g

‡These authors contributed equally to this work.

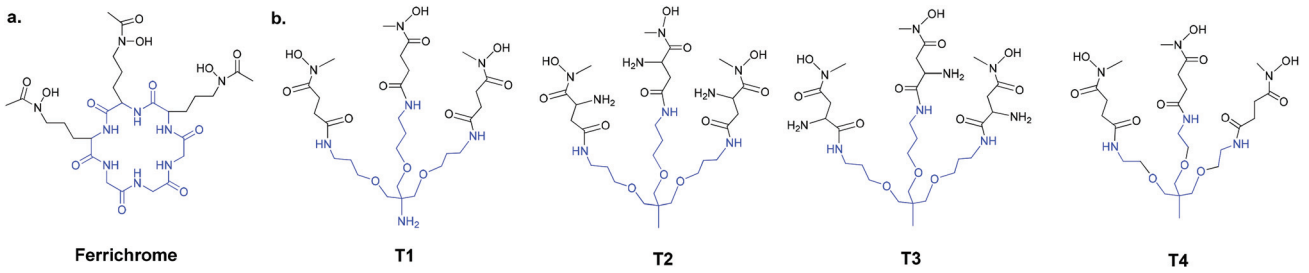

Chart 1 (a) Chemical structure of FC, which consists of a chiral hexapeptide ring (marked in blue) that is non-symmetrically extended by three identical arms terminated by hydroxamate groups. (b) Chemical structure of FC analogs consisting of tris-amino derived templates (marked in blue) extended with succinic acid (**T1** and **T4**) or L/D-Asp (**T2(α)** and **T3(β)**), all terminated by retrohydroxamate groups.

amate moiety (which coordinates the ferric ion in native FC) is an essential feature in the siderophore design. Reversing the directionality of the hydroxamate groups to produce retrohydroxamate (an artificial FC) has little biological effects; the activity of the FC retro-isomer is practically indistinguishable from that of native FC.[34,35]

Initial attempts by our group to mimic FC led to the construction of analogs utilizing simple modular building blocks: a tris-carboxylate derived template extended with chelating arms (based on chiral aliphatic amino acids) and linked to retrohydroxamate.[36–38] This approach had several advantages: (i) synthetic simplicity; (ii) accessibility to enantio-pure iron complexes, which enabled us to explore the transporter's stereo-specific preferences; and (iii) identification of structural motifs on the basic skeleton, such as sites in close proximity to the hydroxamate that can enable narrow-spectrum recognition. However, the low overall number of species-specific analogs capable of promoting bacterial growth, the lack of analogs specific to *E. coli*, and the fact that no analog promoted activity across multiple species, unlike native FC, remained major challenges.

A new approach in designing FC analogs can possibly meet these challenges. In this design, two complementary methodologies can be envisioned. The first is based on developing analogs possessing unsubstituted arms, as in the native FC structure. The second methodology is based on enhancing the H-bonding networks (seen in the high resolution X-ray diffraction analysis of the FhuA transporter with FC)[21,22] by introducing polar side groups that may serve as potential H-donors. Structural optimization of each analog's backbone and improved fitting of the analogs to the FhuA binding site might direct siderophore mimics toward recognition by new bacterial species (particularly *E. coli*) or even provide broad-spectrum recognition. While narrow-spectrum activity offers the potential to develop fast selective diagnostic tools,[39–41] broad-spectrum activity may have therapeutic advantages, as siderophores have no mammalian targets and are therefore non-toxic. Siderophore drug-conjugates might hold the promise of novel antimicrobial agents.[42–46]

The incorporation of succinic or aspartic (Asp) acids into a tris-amino template provides the means for the construction of a small library of FC biomimetics (Chart 1b) whose structures result from the implementation of both proposed methodologies. Coupling succinic acid to the template through one of its carboxyls, while the second is used for the construction of the retrohydroxamate moiety (*via* hydroxylamination) provides a backbone void of substituents on the basic skeleton, as represented by analogs **T1** and **T4**. The incorporation of Asp through its carboxylic acid provides analogs with polar amine side groups. Moreover, the way Asp binds to the template (through the α- or β-carboxyl) provides analogs with the amine at different positions; either α- or β with respect to the hydroxamate moiety and the iron center, as in analogs **T2** and **T3**. Using L/D-Asp in the synthesis of **T2** and **T3** introduces a chiral center into the backbones of the analogs. Since iron is an additional chiral center, diastereomeric pairs for each ligand can be obtained, forming a total of four Asp structural isomers.

This paper describes the synthesis of analogs **T1–T4**, their physicochemical properties, and their growth promotion activity on two reference organisms, *Pseudomonas putida* and *Escherichia coli.* While some derivatives were found to be highly specific for *P. putida*, the succinic acid derivative **T4** showed a broader activity, and was capable of inducing growth in both species. The new tripodal analogs are also compared with other structurally similar analogs in terms of bacterial growth promotion. We also show how systematic modification of their backbones can lead to mimics with broader biological activity.

Results and discussion

Design and synthesis

Two types of tri-amino templates derived from commercially available triols were prepared, both based on a quaternary carbon center connected to three hydroxymethyl groups, which were elongated with either an ethylene (compound **15**) or a propylene (compounds **7** and **11**) spacer (Scheme 1). In compounds **11** and **15**, the fourth substituent on the quaternary carbon (the apical site) was a methyl group. In the case of compound **7**, the inert apical methyl group was replaced by an

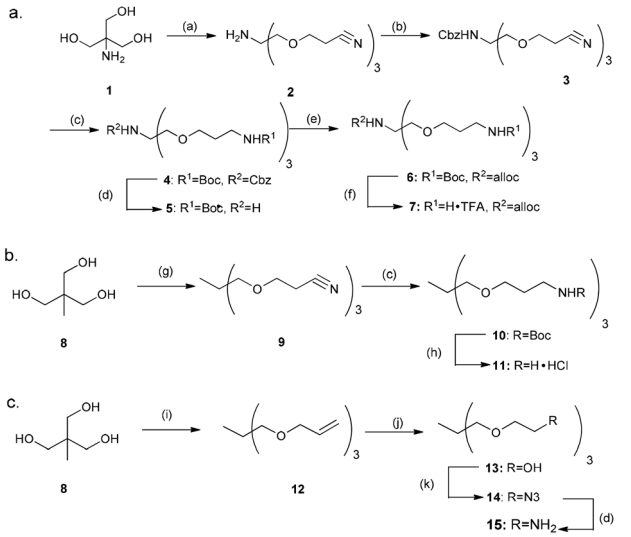

Scheme 1 Synthesis of the tripodal templates **7**, **11** and **15**. Reaction conditions: (a) 40% KOH (aq.), acrylonitrile, dioxane, 0 °C → room temperature (r.t.); (b) 1 M $NaHCO_3$ (aq.), benzyl chloroformate, dioxane 0 °C → r.t.; (c) $CoCl_2{\cdot}6H_2O$, di-*tert*-butyl dicarbonate (Boc), $NaBH_4$, methanol (MeOH), 0 °C → r.t.; (d) 10% Pd/C, H_2, ethanol (EtOH), r.t.; (e) allyl chloroformate, 4 M NaOH (aq.), dioxane, 0 °C → r.t.; (f) 50% trifluoroacetic acid (TFA) in CH_2Cl_2, triisopropylsilane, 0 °C → r.t.; (g) 7.5 M NaOH, acrylonitrile, 0 °C → r.t.; (h) 4 N HCl in dioxane, 0 °C → r.t.; (i) allyl bromide, NaH, DMF, 0 °C → r.t.; (j) O_3, CH_2Cl_2: MeOH, −78 °C. Thiourea, EtOH, $NaBH_4$, 0 °C → r.t.; (k) diphenyl phosphorazide, 1,8-diazabicyclo-[5.4.0]undec-7-ene (DBU), DMF, 0 °C → 50 °C (5 hours) → r.t. For full experimental details, see the ESI.†

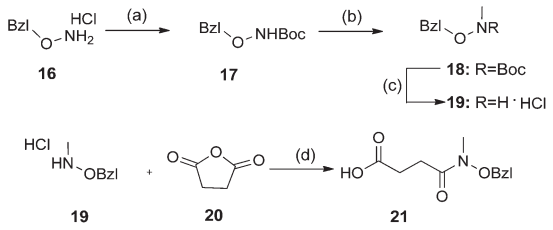

Scheme 2 Synthesis of the succinic acid hydroxamate derivative (the "chelating arm" for analogs **T1** and **T4**). Reaction conditions: (a) Boc, triethylamine (NEt_3), THF/H_2O, r.t.; (b) NaH, methyl iodide, DMF, r.t.; (c) 4 N HCl in dioxane, 0 °C → r.t.; (d) succinic anhydride, K_2CO_3, dioxane, r.t. For full experimental details, see the ESI.†

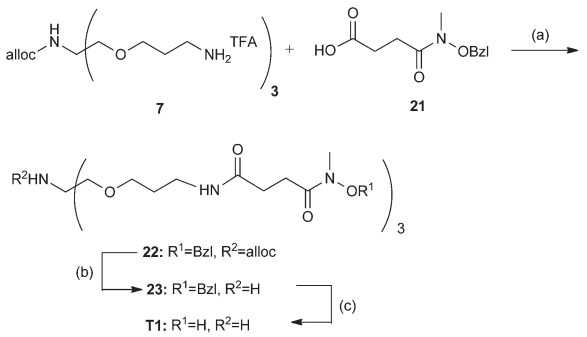

Scheme 3 Synthesis of analog **T1** from the succinic acid hydroxamate derivative **21** and the tripodal template **7**. Reaction conditions: (a) 1-hydroxy-7-azabenzotriazole (HOAt), *N*,*N*′-diisopropylcarbodiimide (DIC), *N*,*N*-diisopropylethylamine (DIPEA), CH_2Cl_2/DMF, r.t.; (b) phenylsilane, $Pd(PPh_3)_4$, CH_2Cl_2, r.t.; (c) 10% Pd/C, H_2, EtOH, r.t. For full experimental details, see the ESI.†

amine group, generating an anchoring point for future introduction of functional conjugates.

Based on the resolved co-crystal structure of FC within the FhuA transporter,[21,22] the iron complex or the FC "head" is embedded in the binding site, while the FC "tail" remains solvent accessible. In similar tripodal templates, the substituted apical site did not interfere with iron-binding or transporter recognition, therefore it was used for coupling fluorescent chromophores for 'signaling',[40,47] or to enable the incorporation of a surface-adhesive moiety.[48]

Templates **7** and **11** (Scheme 1a and b respectively) were prepared by Michael addition of tris(hydroxyme-thyl)aminomethane **1** or 1,1,1-tris(hydroxymethyl)ethane **8** to acrylonitrile,[49,50] followed by the reduction of the trinitrile intermediates using $NaBH_4$ and $CoCl_2$ in the presence of Boc anhydride (*in situ* protection).[51] Acidolysis of Boc provided the desired triamine templates **7** and **11**. The presence of the free functional amine in compound **1** meant that additional synthetic steps were required. The apical amine of compound **2** was protected with carboxybenzyl (Cbz), which is stable under nitrile reductive conditions. After nitrile reduction, Cbz was exchanged with allyloxycarbonyl (alloc),[52] which enabled orthogonal deprotection in later steps of the synthesis.

Template **15**, which has an ethylene spacer (Scheme 1c), was prepared by allylation of triol **8** using allyl bromide.[53] Ozonolysis[53] of **12** and further reduction of the intermediate with $NaBH_4$ provided triol **13**, which was converted to azide **14** using diphenyl phosphorazide, as suggested by Thompson and co-workers.[54] The desired triamine **15** was obtained by hydrogenation of the azide group.

For the synthesis of analogs **T1** and **T4**, the convergent synthetic approach was followed, that is, the template and the chelating arms were prepared separately and only then assembled to generate the desired analog.

The chelating arms were prepared as shown in Scheme 2. The synthesis of *O*-benzyl-*N*-methyl-hydroxylamine **19** was accomplished by bocylation of commercially available *O*-benzyl-hydroxylamine **16** to ensure monomethylation in the next step.[55] Following methylation of **17** by iodomethane,[56] the Boc group was removed by acidolysis.[57] Acetylation of compound **19** with succinic anhydride **20** provided the succinic acid hydroxamate derivative **21**. Compound **21** was coupled through its free carboxyl to the tripodal-triamine template **7** or **15**, providing the protected analogs **22** (Scheme 3) and **25** (Scheme 4), respectively. Removal of the orthogonal protecting groups, alloc and benzyl (Bzl), provided the target compound **T1**, while deprotection of benzyl from **25** provided compound **T4**.

Compounds **T2** and **T3** were prepared in accordance with the principles of linear synthesis, that is, by integrating Asp

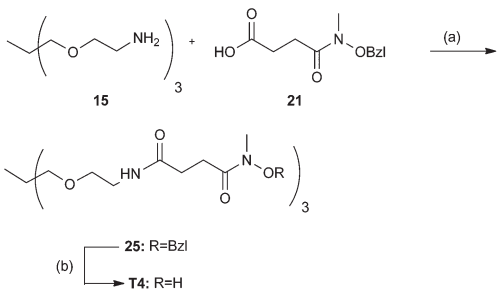

Scheme 4 Synthesis of analog **T4** from the succinic acid hydroxamate derivative **21** and the tripodal template **15**. Reaction conditions: (a) HOAt, DIC, DIPEA, CH_2Cl_2/DMF, r.t.; (b) 10% Pd/C, H_2, EtOH, r.t. For full experimental details, see the ESI.†

into the triamine template and then incorporating *O*-benzyl-*N*-methylhydroxylamine (Scheme 5). This synthetic pathway diminished the tendency of Asp to form the undesired aspartimide by-product.

The two carboxyl groups of Asp could be attached either α or β to the template, generating two analogs differing in the location of the amine side group and chiral center relative to the position of the iron center. Moreover, by using enantiopure L/D-Asp precursors, chiral derivatives were prepared in order to examine their effect on the enantioselective bacterial uptake system.

In this synthetic pathway, the tripodal template **11** was coupled to orthogonally protected Boc-Asp-OBzl **27a** or Boc-Asp-(OBzl)-OH **27b**. Following benzyl deprotection, the intermediates **29a** and **29b** were coupled to *O*-benzyl-*N*-methylhydroxylamine **19**. Acidolysis of Boc and hydrogenolysis of benzyl provided the target compounds **T2** and **T3** as pure L or D isomers.

All compounds were purified by chromatography and characterized using spectroscopic techniques, as fully described in the ESI.†

Physicochemical properties

Binding properties and overall complex stability. Recognition of the ferrisiderophore complex by the bacterial uptake system does not depend on the complex stability constant. However, to function as an efficient iron transporter, a FC analog must be able to form a stable ferric trihydroxamate complex under physiologically relevant pH conditions. Therefore, the pH-dependent distribution of the forms of the FC complexes was obtained, and then the pFe value of each analog, which reflects the efficacy with which it binds ferric iron under the designated conditions, was determined.

In order to determine the stability constants of ferric complexes and to obtain all their coordination characteristics, the acid–base properties of **T1–T4** free ligands were first determined (see the ESI†). Next, electrospray ionization mass spectrometry (ESI-MS) was used to characterize the stoichiometry of the metal complexes in solution. Spectra of the $Fe(ClO_4)_3$/ligand in a 1 : 1 reaction mixture were characterized by the presence of a few major peaks attributable to the mononuclear species (Table S2†).

To determine the stability constants of the **T1–T4** ferric complexes, classical spectrophotometric competition experiments with ethylenediaminetetraacetic acid (EDTA) were performed at pH 8 (Fig. S1†). The overall stability constants, $\log K_{FeL}$, were calculated using eqn (S5) and (S6), the protonation constants of the respective ligands (Table S1†) and of EDTA,[58] and the stability constant of Fe-EDTA.[58] The values obtained for **T1** and **T4** are given in Table 1. However, the **T2** and **T3** ferric complexes exhibited some instability before the equilibrium with EDTA could be achieved and the calculated constants were unreliable (data not shown). A different method, which involved a combination of pH-dependent spectrophotometric and potentiometric titrations, was therefore applied to all the studied compounds. As complex formation for all the studied ligands started at pH of around 0 and the complexation process was complete at pH < 2, the stability constants were determined *via* two series of experiments carried out in a pH range of (i) 0–2 and (ii) 2–8 (Fig. S2†). The $\log K_{FeL}$ values determined from both the EDTA competition and the pH-dependent spectrophotometric/potentiometric titrations are given in Table 1.

Analysis of the pH-dependent distribution of the FC analog complexes provided an understanding of the effect that modifying the structure of the analogs had on their coordination

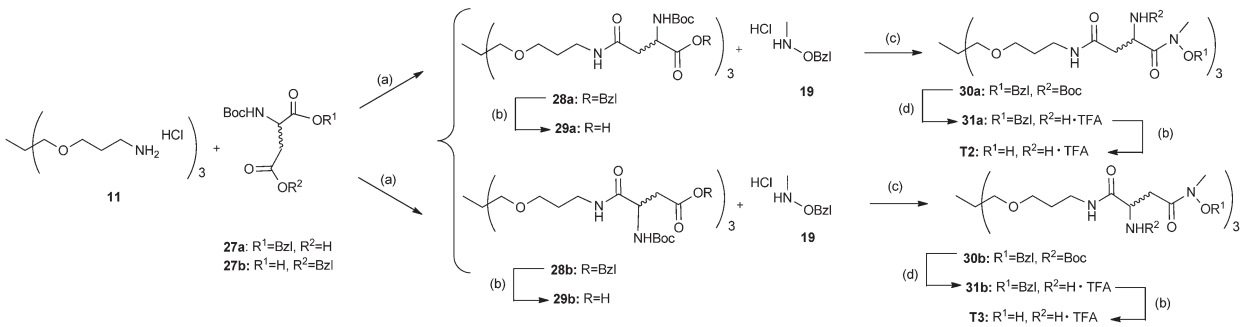

Scheme 5 Synthesis of analogs **T2** and **T3**. Reaction conditions: (a) 1,1′-carbonyldiimidazole (CDI), DIPEA, THF, 0 °C → r.t.; (b) 10% Pd/C, H_2, MeOH, r.t (c) HOAt, DIC, DIPEA, CH_2Cl_2/DMF, r.t.; (d) 50% TFA in CH_2Cl_2, triisopropylsilane, 0 °C → r.t. For full experimental details, see the ESI.†

Table 1 Overall stability constants ($\log K_{FeL}$), $E_{1/2}$ and pFe values for iron(III) complexes[a]

Compound	$\log K_{FeL}$ Fe(III)	Fe(II)	$E_{1/2}$ [mV per NHE]	pFe(III)
FC	29.07[b]	8.5	−446[d]	25.2[b]
T1	27.96(8)[c]	8.9	−360(3)	23.5
	27.45(9)			
T2	27.92(6)	10.0	−289(4)	22.4
T3	26.91(6)	7.9	−356(4)	22.5
T4	27.80(9)[c]	8.3	−390(3)	23.6
	27.34(1)			

[a] Conditions: T = 25 °C, I = 0.10 M $NaClO_4$. [b] Anderegg *et al.*[59] [c] Constants determined from EDTA competition titrations. Conditions: $c_{lig} = c_{Fe(III)} = 1.5 \times 10^{-4}$ M, c_{EDTA} = 0–1.5×10^{-3} M, I = 0.10 M $NaClO_4$. [d] Cooper *et al.*[60]

properties (Fig. S3–S5†). In general, for compounds **T1** and **T4**, two forms, namely dihydroxamate and trihydroxamate, predominated in solution, with the equilibrium between them represented as pK_{NHOH} (Table S3†).

For the **T4** ferric system, pK_{NHOH} was 2.48 and was only slightly higher than the corresponding constant for the **T1** ferric system, 2.32. These two compounds differ in the length of the template spacer and the nature of the apical site ($-CH_3$ *vs.* $-NH_2$). The apical amino group of analog **T1** is too far to influence the di-/trihydroxamate equilibrium, whereas shortening the spacer in the template only slightly affected the binding properties of FC analogs.

In the case of analogs **T2** and **T3**, the presence of external amino substituents in the vicinity of the hydroxamate moieties hampered the formation of the trihydroxamate ferric complexes; the pK_{NHOH} values of 3.40 for **T2** and 2.79 for **T3** were higher than the corresponding value for analog **T1** (Table S3†). Moreover, the presence of charged $-NH_3^+$ groups disturbed the geometry of the di- and trihydroxamate complexes, as was reflected by much lower ε values (Table S4†), and a trihydroxamate complex with the proper octahedral geometry was formed only after their deprotonation (Table S3†). This phenomenon was much more pronounced in analog **T2**, and resulted from the charge and electronic effects of the protonated amino groups located in close proximity to the hydroxamate functional groups.

CV (cyclic voltammetry) measurements. In order to study the redox chemistry of FC analogs, electrochemical measurements were performed. For ferric complexes of **T1–T4**, quasi-reversible voltammograms were obtained (Fig. S6†), with ΔE in the range of 95–135 mV. The values of $E_{1/2}$ were recalculated *vs.* normal hydrogen electrode (NHE) and are presented in Table 1. Overall, in comparison with FC, the ferric complexes of **T1–T4** ligands presented a less negative redox potential, reflecting their lower stability (*vide supra*). The approximate stability constants of ferrous Fe(II)L complexes, calculated using eqn (S10) and the $\log K_{Fe(III)L}$ from Table 1, were around 20 orders of magnitude lower than the stability constants for the corresponding ferric complexes, which is in agreement with the behavior of hydroxamate siderophores.

pFe of ferric complexes. To compare the efficacy of iron chelation by the studied ligands with that of other trihydroxamate-based natural or synthetic siderophores, the free hexaaquairon(III) concentrations were calculated (pFe = $-\log [Fe(III)_{(aq)}]$ at a pH of 7.4 with a total ligand concentration of 10^{-5} M and a total Fe(III) concentration of 10^{-6} M).[61] The results (Table 1) clearly demonstrated that shortening the template backbone by one methylene group did not affect the binding properties of the molecule (pFe of 23.5 *vs.* 23.6 for **T1** and **T4**, respectively), whereas the introduction of amino groups as external substituents on the basic backbone slightly decreased the Fe(III) binding efficacy (pFe of 22.4 *vs.* 22.5 for **T2** and **T3**, respectively). Therefore, even if the amino groups were deprotonated and uncharged at pH 7.4, they still induced steric hindrance, lowering the pFe by around one order of magnitude. Generally, the pFe values for the non-substituted analogs were less than two orders of magnitude lower than the pFe values of natural FC, while those for the amino-substituted analogs were almost three orders of magnitude lower. Nevertheless, the pFe values for all the studied tripodal FC analogs remained within the range for effective iron chelators (Table S5†).

CD (circular dichroism) of ferric complexes. The chiral preferences of the **T2** and **T3** ferric complexes in solution were determined by CD. L- and D-**T2** complexes displayed spectra (Fig. 1) corresponding to tris-hydroxamate ferric complexes, with a typical ligand-to-metal charge transfer (LMCT) band in the region of 420 nm.[62,63] As expected, L- and D-diastereomers displayed opposite spectral configurations: a right handed-Δ configuration in the case of L-Asp, and a left handed-Λ configuration in the case of D-Asp acid derivatives. Both the D-analog and the native FC[63] preferably formed left handed-Λ iron complexes.

Although both **T2** and **T3** were expected to exhibit a chiral preference, L- and D-**T3** presented a negligible CD signal (data not shown). By contrast, the presence of chiral centers near the iron binding site (α position) in **T2** induced a larger energy difference between the Δ and Λ configurations, with a preference for the more stable form.[64] Compared with **T2**, the chiral center in compound **T3** was located farther from the iron

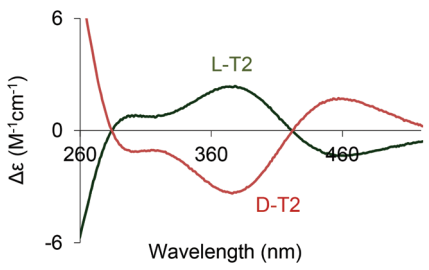

Fig. 1 CD spectra of L- and D-**T2** ferric complexes. Solvent: tris/$HClO_4$ buffer (pH = 7.8, I = 0.1 M $NaClO_4$). Complex concentration of 0.25 mM.

binding site (β position). Moving of the chiral center away from the chirogenic octahedral iron center (even by a single carbon) practically abolishes chiral discrimination, thus leading practically to a racemic mixture of Δ and Λ configurations of **T3**.

Examination of the biological activity of the FC analogs. The synthetic siderophore analogs were tested on two microorganisms: *Pseudomonas putida* mutant JM218, provided by L. C. van Loon, Utrecht, the Netherlands;[40] and *Escherichia coli* mutant UT5600,[65] obtained from the Coli Genetic Stock center. These mutants possess transporters for FC but do not produce their own siderophores; therefore, no exchange can occur between heterologous and native siderophores. The growth of these strains is proportional to the bio-availability of ferric complexes.

The growth-promoting effects of the synthetic analogs were compared with each other (Table 2) and with natural FC (positive control) and double-distilled water (DDW; negative control). The siderophore iron-complexes were added to the growth medium as the sole iron source. To remove iron traces, modified King's B (MKB) medium was treated with the amidoxime-chelating resin Purolite® S910. Bacteria were inoculated in iron-depleted MKB liquid medium and incubated at 30 °C until the bacterial stationary phase. Their growth was followed by measuring their optical density at 600 nm at fixed time intervals. Each enantiomer was tested separately (for full experimental procedures, see the ESI†).

A comparison of the uptake by *P. putida* and *E. coli* (Fig. S7 and S8†) indicated that both bacterial strains were able to consume artificial siderophores in addition to FC (Table 2). Compound **T1** was only recognized by *P. putida*, however, a slightly modified template, substituted with an ethylene spacer instead of the propylene spacer and bearing methyl instead of amine on the apical site, produced a new analog **T4**, with excellent growth enhancement properties in both *P. putida* and *E. coli.* Further improvement was obtained by

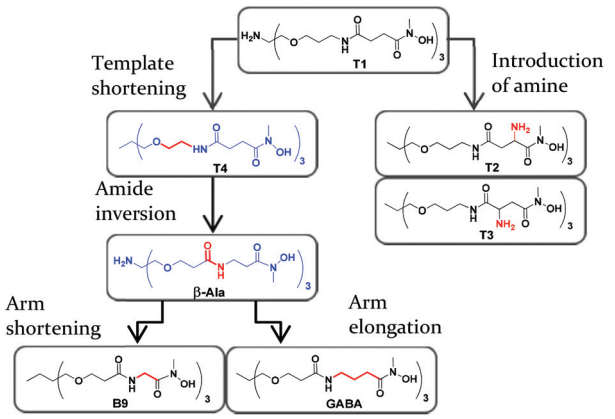

Chart 2 Representation of the systematic modification performed on the backbones of the FC analogs. Modifications to the analog backbone are marked in red. Compounds able to promote the growth of both *E. coli* and *P. putida* are shown in blue.

reversing the direction of the amide linkage to produce an analog (**β-Ala**) that promoted growth to the same extent as FC in both *P. putida* and *E. coli* (Table 2, and Chart 2). **β-Ala**, like analog **T1**, possesses an apical amino group, however the different recognition of **T1** and **β-Ala** indicates that this group is not a key structural feature, and that the amine "tail" most likely does not interact with the recognition domain of the FhuA transporter. Analogs **T4** and **β-Ala** were able to match the FhuA transporter in that they could effectively promote the growth of dissimilar microorganisms. Such broad-spectrum activity, similar to that of FC, is rare among synthetic analogs.

Extending the arm with a propylene spacer, as in the **GABA** analog, or shortening the arm to a single methylene spacer, as in **B9**, had no effect on *P. putida* propagation, while completely abolishing *E. coli* growth (Table 2, and Chart 2).

Optimal recognition by *E. coli* was achieved for analogs with backbones having ethylene spacers in both the template and the arms, indicating the need to retain well-defined distances in both the arms and the template. The fact that some analogs failed to transport iron to *E. coli*, while being fully active in *P. putida*, suggests that the FC uptake systems of these two bacterial strains are not identical.

Our attempt to enhance the H-bonding network in the recognition-domain of FhuA by developing analogs carrying amine side groups (**T2** and **T3**) produced analogs that facilitated growth in *P. putida* but not in *E. coli*. It seems that the recognition domain in *P. putida* is more tolerant (possibly less crowded) than that of *E. coli*, as it was shown to tolerate aliphatic side groups as well as polar amine substituents.[38] The location of the amine group one position farther from the metal binding site (*i.e.*, in the β position with respect to the iron center) improved *P. putida* recognition from high to full activity (Table 2, **T2** and **T3**, respectively).

The observation that there was no difference between the growth promoting effects of the enantiomer pairs of **T2** and **T3** (Λ and Δ isomers) *vis-à-vis P. putida* is quite puzzling, given

Table 2 Biological activity of the artificial siderophores in *P. putida* (JM218) and *E. coli* (UT5600)

Compound	Growth promotion[a]		
	E. coli[b]	*P. putida*[b]	Reference
FC	+++++	+++++	Current work
T1	–	+++++	Current work
L/D-**T2**	–	++++	Current work
L/D-**T3**	–	+++++	Current work
T4	++++	+++++	Current work
β-Ala[c]	+++++	+++++	Besserglick *et al.*[66]
GABA[c]	–	+++++	Besserglick *et al.*[66]
B9[c]	–	+++++	Jurkevitch *et al.*[38]
DDW	–	–	Current work

[a] Scale from full activity (+++++) to no activity (–) based on the optical density at 600 nm in comparison with that of positive (FC) and negative (DDW) controls. [b] The results represent the stationary phase of the appropriate bacterial strain. [c] See Chart 2 for the structures of **GABA**, **β-Ala**, and **B9**.

that this result is in direct contrast to the enantioselectivity of FC[67,68] and of similar artificial chiral siderophores.[64] The lack of stereospecificity observed in analogs **T2** and **T3** may reflect the lability of iron-complexes with respect to isomerization in aqueous solutions.[24] Ligand exchange can shift complexes possessing a Δ-configuration to the FhuA-preferred Λ-configuration, thus allowing utilization of both isomers. An alternative possibility is that several distinct siderophore transporters participate in the transport of different isomers (*e.g.* FhuA in the transport of the Λ-isomer and FhuE[69] in the transport of the Δ-isomer). It is, however, unlikely that different transporters will generate growth promotion curves with practically identical kinetic parameters (Fig. S8†).

The extent to which transport is governed exclusively by a single transporter has been addressed in previous studies and in this work. We have previously shown, by radioactive competition uptake assays, that the uptake of tripodal analogs in *P. putida* is primarily carried out through the FC transporter.[38,64] In a similar experiment, Schalk suggested that *P. aeruginosa* takes-up the tripodal artificial analog and native FC with equal efficiency.[70]

The uptake and release pathway in *E. coli* UT5600 was studied using fluorescent tripodal **β-Ala** labeled with naphthalimide (see the ESI†). The bound iron(III) quenches the fluorophore emission, once the iron is taken-up in the cytosol the green fluorescence is restored and the distribution of the iron-free siderophore recorded. In the case of *E. coli* K-12, which lacks an external transporter (the ΔfhuA mutant obtained from the Coli Genetic Stock center),[71] no fluorescence was observed, indicating that uptake is exclusively carried out by the FhuA receptor (Fig. S9†).

Summary and conclusions

FC is an attractive model for studies since a detailed X-ray structure of FhuA[21,22] is available, so allowing researchers to focus attention on the parameters important for transporter recognition. The X-ray structure shows two sets of H-bonding interactions between FC and the FhuA transporter. One set involves the hydroxamate oxygens and the second set involves carbonyls on the peptide backbone. We assumed that the H-bonding interactions with hydroxamate or retrohydroxamate are practically identical. Thus, the only accessible means to match the remaining H-bonding and control the analog's overall size was *via* the spacers. Spacers inserted into the template backbone and/or the arms can optimize the directionality and the relative orientation of the functional groups involved in H-bonding. Alternatively, additional H-donor groups, such as external amines, can be introduced to try to enhance the H-bonding network.

Here, we present a new series of FC analogs. The series utilizes two C3 symmetric tris-amino derived templates extended by succinic (**T1** and **T4**) or Asp (**T2** and **T3**) acids, with all compounds terminated by retrohydroxamates. The resulting FC analogs differ with respect to their skeletal lengths and compositions, with analogs **T2** and **T3** substituted by amine side-groups. In addition, we present a synthetic methodology for introducing functional-conjugates at the template's apical site to allow future therapeutic applications, as represented by analog **T1**.

The iron-complex formation characteristics and stability of the analogs were investigated in detail. All the investigated FC analogs bind ferric ions in a 1 : 1 stoichiometry, as demonstrated by ESI-MS and further confirmed by potentiometric and spectrophotometric monitoring. Chiral preferences were investigated by CD. Chiral centers located near the metal binding site display LMCT bands with Δ and Λ configurations typical for trishydroxamate-ferric complexes. However, distancing the chiral center from the metal binding site practically abolishes chiral discrimination. The affinities of the iron-siderophores, as reflected by pFe, show that the ferric complexes of all the presented analogs are about 1–2 orders of magnitude less stable than those of FC. Although the amine substituents are located in close proximity to the metal binding site, the amines are not involved in iron coordination. The external amine substituents slightly destabilize the ferric complex, most likely due to electrostatic repulsion between the neighboring arms, thus preventing the formation of the stabilizing H-bonds observed in native FC.[63] Nevertheless, the stability of all the complexes lies within the range of natural siderophores,[7,24,72] and therefore these FC analogs can be utilized as potent siderophores.

The biological potency of the new analogs was monitored by growth promotion experiments. The analogs exhibit biological activities that can be divided into two sub-groups: one (**T1–T3**) that shows high specificity toward *P. putida*, but are not recognized by *E. coli*; and another (**T4**) that is recognized by both *P. putida* and *E. coli.* The existence of the first group indicates that the FC recognition domains of these two bacteria differ considerably, whereas the second group shows that the simple platform of ethylene-amide-ethylene-retrohydroxamate is capable of matching different transporters in dissimilar microorganisms, as does the native FC.

The less-tolerant structure of the *E. coli* transporter compared with the accommodating structure of the *P. putida* transporter allows us to establish the minimal essential structural parameters for broad-spectrum recognition; an elusive target that we and others have been pursuing for years. The governing rules for designing analogs with multiple-uptake capabilities are: (i) to mimic the transporter with the most stringent requirements, such as the FhuA transporter in *E. coli*; (ii) to develop a library of analogs in which each building group can be systematically and gradually modified until optimization is obtained, as was demonstrated through step-by-step structural adjustments of the modular system described in this work. It should be noted that minor modification may abolish broad-spectrum activity, so inducing the formation of narrow-spectrum analogs utilizing practically the same platform.

Although we have not identified an artificial analog targeting exclusively *E. coli*, understanding the unique requirements of FhuA may facilitate its preparation. The interactions

between FC and its transporter may serve as a prototype for other hydroxamate siderophores for which the detailed X-ray structure is lacking. Assuming similar H-bonding interactions to those described for FC in its transporter, we suggest following similar optimization processes.

In future work, we will try to extend the guidelines for optimization and multiple-recognition to other bacteria and other siderophores with an emphasis on mammalian pathogenic targets. We also plan to initiate a computer 'docking' analysis aimed at understanding the origin of recognition in *E. coli* and at resolving the lack of stereo-specificity observed in both enantiomer pairs derived from Asp in *P. putida*.

Acknowledgements

E. G.-K. and A. Sz. are grateful to the Polish National Science Center (NCN, UMO-2011/03/B/ST5/01057) and Wroclaw Centre of Biotechnology (The Leading National Research Centre Program, KNOW, 2014–2018) for financial support.

References

1 J. B. Neilands, *Annu. Rev. Nutr.*, 1981, **1**, 27.
2 C. Wandersman and P. Delepelaire, *Annu. Rev. Microbiol.*, 2004, **58**, 611.
3 M. L. Guerinot, *Annu. Rev. Microbiol.*, 1994, **48**, 743.
4 J. B. Neilands, *J. Biol. Chem.*, 1995, **270**, 26723.
5 G. Winkelmann, *Biochem. Soc. Trans.*, 2002, **30**, 691.
6 C. Ratledge and L. G. Dover, *Annu. Rev. Microbiol.*, 2000, **54**, 881.
7 R. C. Hider and X. Kong, *Nat. Prod. Rep.*, 2010, **27**, 637.
8 I. J. Schalk, G. L. A. Mislin and K. Brillet, in *Current Topics in Membranes*, ed. J. M. Arguello and S. Lutsenko, Elsevier, 2012, vol. 69, ch. 2, p. 37.
9 I. J. Schalk and L. Guillon, *Amino Acids*, 2013, **44**, 1267.
10 K. D. Krewulak and H. J. Vogel, *Biochim. Biophys. Acta*, 2008, **1778**, 1781.
11 M. Miethke and M. A. Marahiel, *Microbiol. Mol. Biol. Rev.*, 2007, **71**, 413.
12 V. Braun and K. Hantke, in *Microbial transport systems*, ed. G. Winkelmann, Wiley-VCH, Weinheim, 2002, ch. 12, p. 289.
13 V. Braun and H. Killmann, *Trends Biochem. Sci.*, 1999, **24**, 104.
14 J. B. Neilands, *J. Am. Chem. Soc.*, 1952, **74**, 4846.
15 S. J. Rogers, R. A. Warren and J. B. Neilands, *Nature*, 1963, **200**, 167.
16 J. B. Neilands, *Science*, 1967, **156**, 1443.
17 D. E. Crowley, Y. C. Wang, C. P. P. Reid and P. J. Szaniszlo, *Plant Soil*, 1991, **130**, 179.
18 E. Barness, Y. Hadar, Y. Chen, A. Shanzer and J. Libman, *Plant Physiol.*, 1992, **99**, 1329.
19 R. Chakraborty, E. Storey and D. van der Helm, *Biometals*, 2007, **20**, 263.
20 D. van der Helm and R. Chakraborty, in *Microbial transport systems*, ed. G. Winkelmann, Wiley-VCH, Weinheim, 2002, ch. 11, p. 261.
21 A. D. Ferguson, E. Hofmann, J. W. Coulton, K. Diederichs and W. Welte, *Science*, 1998, **282**, 2215.
22 K. P. Locher, B. Rees, R. Koebnik, A. Mitschler, L. Moulinier, J. P. Rosenbusch and D. Moras, *Cell*, 1998, **95**, 771.
23 R. Breslow, *Chem. Soc. Rev.*, 1972, **1**, 553.
24 K. N. Raymond, G. Muller and B. F. Matzanke, *Top. Curr. Chem.*, 1984, **123**, 49.
25 A. Shanzer, C. E. Felder and Y. Barda, in *The Chemistry of Hydroxylamines, Oximes and Hydroxamic Acids*, ed. Z. Rappoport and J. F. Liebman, John Wiley & Sons, Ltd, 2009, ch. 16, p. 751.
26 M. J. Miller, *Chem. Rev.*, 1989, **89**, 1563.
27 S. Heggemann, U. Mollmann, P. Gebhardt and L. Heinisch, *Biometals*, 2003, **16**, 539.
28 M. Gaspar, M. A. Santos, K. Krauter and G. Winkelmann, *Biometals*, 1999, **12**, 209.
29 S. K. Sharma, M. J. Miller and S. M. Payne, *J. Med. Chem.*, 1989, **32**, 357.
30 S. Dhungana, J. M. Harrington, P. Geblhardt, U. Mollmann and A. L. Crumbliss, *Inorg. Chem.*, 2007, **46**, 8362.
31 B. H. Lee, M. J. Miller, C. A. Prody and J. B. Neilands, *J. Med. Chem.*, 1985, **28**, 317.
32 B. H. Lee, M. J. Miller, C. A. Prody and J. B. Neilands, *J. Med. Chem.*, 1985, **28**, 323.
33 K. Matsumoto, T. Ozawa, K. Jitsukawa and H. Masuda, *Inorg. Chem.*, 2004, **43**, 8538.
34 T. Emery, L. Emery and R. K. Olsen, *Biochem. Biophys. Res. Commun.*, 1984, **119**, 1191.
35 R. K. Olsen and K. Ramasamy, *J. Org. Chem.*, 1985, **50**, 2264.
36 A. Shanzer, J. Libman, R. Lazar and Y. Tor, *Pure Appl. Chem.*, 1989, **61**, 1529.
37 A. Shanzer, J. Libman, R. Lazar, Y. Tor and T. Emery, *Biochem. Biophys. Res. Commun.*, 1988, **157**, 389.
38 E. Jurkevitch, Y. Hadar, Y. Chen, J. Libman and A. Shanzer, *J. Bacteriol.*, 1992, **174**, 78.
39 O. Ardon, R. Nudelman, C. Caris, J. Libman, A. Shanzer, Y. Chen and Y. Hadar, *J. Bacteriol.*, 1998, **180**, 2021.
40 H. Weizman, O. Ardon, B. Mester, J. Libman, O. Dwir, Y. Hadar, Y. Chen and A. Shanzer, *J. Am. Chem. Soc.*, 1996, **118**, 12368.
41 T. Zheng and E. M. Nolan, *Metallomics*, 2012, **4**, 866.
42 M. J. Miller, J. A. Mckee, A. A. Minnick and E. K. Dolence, *Biol. Met.*, 1991, **4**, 62.
43 U. Mollmann, L. Heinisch, A. Bauernfeind, T. Kohler and D. Ankel-Fuchs, *Biometals*, 2009, **22**, 615.
44 C. Ji, R. E. Juarez-Hernandez and M. J. Miller, *Future Med. Chem.*, 2012, **4**, 297.
45 J. M. Roosenberg, Y. M. Lin, Y. Lu and M. J. Miller, *Curr. Med. Chem.*, 2000, **7**, 159.

46 S. J. Milner, A. Seve, A. M. Snelling, G. H. Thomas, K. G. Kerr, A. Routledge and A. K. Duhme-Klair, *Org. Biomol. Chem.*, 2013, **11**, 3461.
47 R. Nudelman, O. Ardon, Y. Hadar, Y. N. Chen, J. Libman and A. Shanzer, *J. Med. Chem.*, 1998, **41**, 1671.
48 Y. Gafni, H. Weizman, J. Libman, A. Shanzer and I. Rubinstein, *Chem. – Eur. J.*, 1996, **2**, 759.
49 G. R. Newkome, X. F. Lin and J. K. Young, *Synlett*, 1992, 53.
50 R. Kikkeri, H. Traboulsi, N. Humbert, E. Gumienna-Kontecka, R. Arad-Yellin, G. Melman, M. Elhabiri, A. M. Albrecht-Gary and A. Shanzer, *Inorg. Chem.*, 2007, **46**, 2485.
51 S. Caddick, A. K. D. Haynes, D. B. Judd and M. R. V. Williams, *Tetrahedron Lett.*, 2000, **41**, 3513.
52 C. M. Stevens and R. Watanabe, *J. Am. Chem. Soc.*, 1950, **72**, 725.
53 S. Hanessian, H. Prabhanjan, D. X. Qiu and S. Nambiar, *Can. J. Chem.*, 1996, **74**, 2540.
54 A. S. Thompson, G. R. Humphrey, A. M. Demarco, D. J. Mathre and E. J. J. Grabowski, *J. Org. Chem.*, 1993, **58**, 5886.
55 B. H. Lee and M. J. Miller, *J. Org. Chem.*, 1983, **48**, 24.
56 R. Grigg, Z. Rankovic and M. Thoroughgood, *Tetrahedron*, 2000, **56**, 8025.
57 G. Han, M. Tamaki and V. Hruby, *J. Pept. Res.*, 2001, **58**, 338.
58 L. D. Pettit and H. K. Powell, Timble, York, UK, 2001, (http://www.acadsoft.co.uk, version 5.6).
59 G. Anderegg, F. L'Eplattenier and G. Schwarzenbach, *Helv. Chim. Acta*, 1963, **46**, 1409.
60 S. R. Cooper, J. V. Mcardle and K. N. Raymond, *Proc. Natl. Acad. Sci. U. S. A.*, 1978, **75**, 3551.
61 W. R. Harris, C. J. Carrano, S. R. Cooper, S. R. Sofen, A. E. Avdeef, J. V. Mcardle and K. N. Raymond, *J. Am. Chem. Soc.*, 1979, **101**, 6097.
62 K. N. Raymond and C. J. Carrano, *Acc. Chem. Res.*, 1979, **12**, 183.
63 D. Van der Helm, J. R. Baker, D. L. Engwilmot, M. B. Hossain and R. A. Loghry, *J. Am. Chem. Soc.*, 1980, **102**, 4224.
64 A. Shanzer, J. Libman, P. Yakirevitch, Y. Hadar, Y. Chen and E. Jurkevitch, *Chirality*, 1993, **5**, 359.
65 M. E. Elish, J. R. Pierce and C. F. Earhart, *J. Gen. Microbiol.*, 1988, **134**, 1355.
66 J. Besserglick, *Thesis for the degree Doctor of Philosophy*, Weizmann Institute of Science, 2013.
67 G. Winkelmann, *FEBS Lett.*, 1979, **97**, 43.
68 G. Winkelmann and V. Braun, *FEMS Microbiol. Lett.*, 1981, **11**, 237.
69 M. Sauer, K. Hantke and V. Braun, *J. Bacteriol.*, 1987, **169**, 2044.
70 M. Hannauer, Y. Barda, G. L. A. Mislin, A. Shanzer and I. J. Schalk, *J. Bacteriol.*, 2010, **192**, 1212.
71 T. Baba, T. Ara, M. Hasegawa, Y. Takai, Y. Okumura, M. Baba, K. A. Datsenko, M. Tomita, B. L. Wanner and H. Mori, *Mol. Syst. Biol.*, 2006, 2.
72 H. Boukhalfa and A. L. Crumbliss, *Biometals*, 2002, **15**, 325.